


J.-P. BESSON¹,
S. SCHILT²
L. THÉVENAZ¹

Molecular relaxation effects in hydrogen chloride photoacoustic detection

¹ Ecole Polytechnique Fédérale de Lausanne (EPFL), Nanophotonics and Metrology Laboratory, 1015 Lausanne, Switzerland

² IR Microsystems, PSE-C, 1015 Lausanne, Switzerland

Received: 14 September 2007

Published online: 15 November 2007 • © Springer-Verlag 2007

ABSTRACT A photoacoustic (PA) sensor has been developed to monitor hydrogen chloride at sub-ppm level in the 1740-nm region. The system was designed to control the process in the novel low-water-peak optical fiber manufacturing process. Relaxation effects in hydrogen chloride PA detection in oxygen–helium and nitrogen–helium gas mixtures are presented, showing that the generation of the PA signal is strongly affected by the ratio of these substances. In addition, the role of water vapor in the PA signal is investigated.

PACS 42.62.Fi; 78.20.Hp; 34.50.Ez

1 Introduction

Photoacoustic spectroscopy (PAS) is a widely recognized technique for its high performance in the detection of trace gases in various applications [1–3]. The main advantages of this technique are its intrinsically zero background nature and its achromaticity, which result in a very sensitive and simple setup arrangement suitable in a broad spectral region ranging from the ultraviolet to the mid infrared.

The development of photoacoustic (PA) sensors operating in the near-infrared (NIR) range has strongly increased in recent years due to the excellent properties of the available diode lasers. Such laser sources provide single-mode emission (for instance distributed feedback (DFB) lasers) with narrow line width (typically a few MHz), an output power ranging from a few mW to several tens of mW, modulation capabilities and thousands of hours of operation. Moreover, their compact size and their fiber-coupled output make them easy to align with the PA cell.

Despite its above-mentioned advantages, PAS is an indirect method since the optical energy absorbed by the molecules is detected through an acoustic wave generated in the gas due to thermal expansion resulting from the vibration-to-translation (V–T) relaxation of the excited molecules. Consequently, the conversion from optical to thermal energy depends on the physico-thermal properties of the gas, so that a calibration of the sensor is required. Whereas molecular re-

laxation of the excited rovibrational state is assumed to be instantaneous in most cases, some particular gas mixtures result in a much slower process. In this case, the PA signal is strongly influenced by this phenomenon and requires a precise analysis.

Molecular relaxation effects have been described in the NIR for the detection of methane (CH₄) [4], carbon dioxide (CO₂) [5] and hydrogen cyanide (HCN) [6]. In this paper, we report the influence of molecular relaxation on hydrogen chloride (HCl) detection in different gas mixtures containing helium (He). HCl is an important indicator of gas purity in the manufacturing of the new zero-water-peak fibers used in optical telecommunication networks [7]. The manufacturing of the fiber preform is usually made by modified chemical vapor deposition and the carrier gas used in this process mainly consists of a mixture of oxygen (O₂) and helium. Thus, HCl is detected in a specific mixture made of these two compounds. In addition, the effect of nitrogen (N₂) on HCl detection is also investigated. Finally, the effect of water vapor (H₂O) playing the role of a catalyst in the PA signal is described.

2 Experimental details

A fiber-coupled PA sensor based on a resonant configuration has been developed to detect HCl. Details of the sensor architecture and performances can be found in [8]. The PA cell consists of three parallel resonators enabling the possibility to measure up to three different gases using three lasers, but only one resonator has been used in the present work (Fig. 1). The PA sensor is operated in its first longitudinal mode with a resonant frequency around 1 kHz in air. A sensitive electret microphone located at the center of the resonator is used to detect the acoustic wave. After amplification, the PA signal is measured using a lock-in amplifier with a time constant usually set to 10 s. Finally, the PA signal is recorded by a computer.

A pigtailed DFB laser tuned to 1738.9 nm is used to probe the R4 HCl line in the 2ν band. The temperature and current tuning coefficients of the laser are respectively –12.5 GHz/°C and –0.86 GHz/mA and the average power at the output of the fiber is 16 mW in the typical operating conditions. The laser is connected to a fiber collimator which is properly aligned along the cell axis to avoid any additional acoustic noise (wall noise).

✉ Fax: +41-21-693-2614, E-mail: jean-philippe.besson@epfl.ch

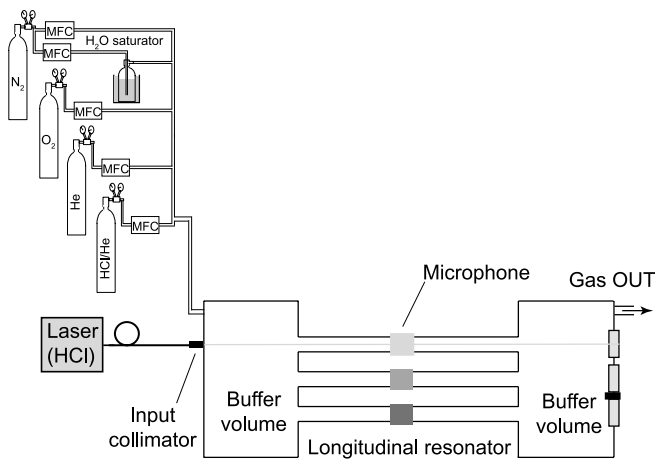


FIGURE 1 Scheme of the experimental setup including the PA cell and the gas-mixing system made of four mass-flow controllers (MFCs), certified cylinders and a water-vapor saturator

The laser is current modulated at the resonance frequency with a square waveform of proper amplitude in order to induce wavelength modulation (WM). More details about the modulation scheme are given in Sect. 3.1.

Various HCl concentrations and carrier gas compositions have been prepared from certified cylinders using mass-flow controllers (MFCs). A cylinder of 50 ppm HCl buffered in He and pure gases (N_2 , O_2 and He) have been used to perform the measurements. A total flow rate of 500 sccm (standard cubic centimeters per minute) and a constant dilution of 5 ppm HCl were used to point out molecular relaxation effects. In addition, water vapor could be added to the final gas mixture by bubbling part of the flow into a water-filled glass cuvette placed in a thermostat bath. All the measurements were performed at atmospheric pressure.

3 Results and discussion

3.1 Normalization of the PA signal

In order to observe relaxation effects of HCl in He– N_2 and He– O_2 gas mixtures, different ratios of He/ N_2 and He/ O_2 were considered as a buffer gas. However, the variation of the He/ N_2 and He/ O_2 percentages has additional effects on the PA signal besides relaxation effects. In particular, the buffer gas influences the resonance frequency, the quality factor and the cell constant, which are directly related to the PA signal. For instance, the resonance frequency changed from about 1000 Hz in N_2 to 2700 Hz in He. Moreover, the sensitivity of the microphone is frequency dependent and the foreign-broadening coefficient of the considered HCl absorption line is different in helium than in oxygen or nitrogen. In order to isolate the contribution of molecular relaxation from other effects, a normalization of the PA signal has been used.

The basic target of this normalization was to compensate as much as possible the variation of the HCl PA signal in the different buffer gases that was not induced by relaxation effects. For this purpose, the PA signal measured for HCl has been compared to the signal induced by another species that is not subject to molecular relaxation in the considered gas mixtures. Water vapor has thus been selected, since no relaxation effects occur for this substance at sufficiently high concentra-

tion [9]. The water-vapor PA signal was recorded in the same gas mixtures (N_2 /He and O_2 /He of different mixing ratios) as used for HCl measurement. A concentration of 1% of H_2O was measured using a 1369-nm DFB laser. Wavelength modulation was applied to both lasers through a modulation of the laser injection current with a fixed amplitude optimized to maximize the PA signal in air for H_2O and in a 50% O_2 –50% He mixture for HCl. This amplitude was then kept fixed during all measurements, whereas the direct current was slightly adjusted to maximize the PA signal.

Results of H_2O measurements are presented in Fig. 2. The obtained curves were then used for the normalization of the HCl PA signal measured in the same gas mixtures. This normalization takes into account the effects of the buffer on the quality factor, on the resonance frequency and on the microphone response. However, additional effects due to different line-broadening parameters were not corrected with this normalization. For instance, the broadening coefficient of the water-vapor absorption line is dependent on the buffer gas and is different from the broadening coefficient of the considered HCl absorption line. Therefore, a theoretical investigation through simulations was performed to estimate the error induced by the line broadening in the normalization process. A simulation of the WM-generated PA signals of HCl and H_2O was performed for this purpose. The simulation considered a Lorentzian line shape function and pure wavelength modulation of the laser, i.e. neglecting the residual amplitude modulation associated with the laser current modulation [10]. The effect of the normalized WM index $m = \Delta\nu/\Delta\nu_r$ [11] was also taken into account, where $\Delta\nu$ is the frequency deviation of the optical carrier and $\Delta\nu_r$ is the absorption line width. The WM index depends on the gas composition, since the width of the line changes, which produces a variation of the PA signal.

Foreign-broadening coefficients due to He, O_2 and N_2 are required in the simulations for both HCl and H_2O lines in order to evaluate the error in the normalization process induced by the different broadenings. However, these coefficients are not known for the considered transitions. Therefore, estimated values have been considered based on results reported in the literature for other HCl and H_2O lines at a close wavelength. For HCl, He-, N_2 - and O_2 -broadening coefficients are reported for the nearby R3 line located at

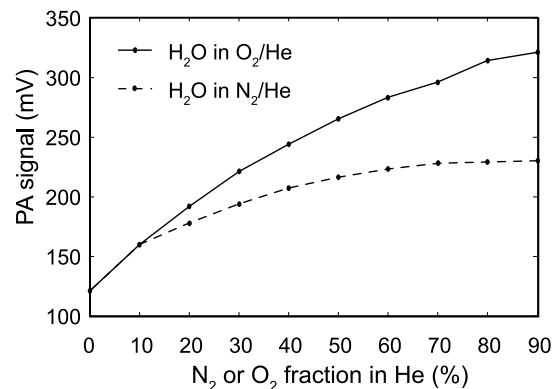


FIGURE 2 Normalization curves performed in H_2O diluted in a mixture of N_2 –He (dashed curve) and in a mixture of O_2 –He (solid curve). The variation of the PA signal is mainly due to the difference in the line-broadening coefficients of H_2O in O_2 and in N_2

	Measurements		Simulations	
	H ₂ O	HCl	H ₂ O	HCl
λ (nm)	1368.7	1738.9	1393.5	1742.4
Identification	See ^a	R4	See ^b	R3
Strength (cm ⁻¹ /(mol cm ⁻²))	1.01×10^{-21}	9.67×10^{-21}	2.72×10^{-22}	1.16×10^{-20}
γ_{air} (cm ⁻¹ atm ⁻¹)	0.093	0.0537	0.0958	0.0624
γ_{self} (cm ⁻¹ atm ⁻¹)	0.51	0.2178	0.488	0.2408
γ_{He} (cm ⁻¹ atm ⁻¹)	–	–	0.0221	0.0221
γ_{N_2} (cm ⁻¹ atm ⁻¹)	–	–	0.1130	0.0753
γ_{O_2} (cm ⁻¹ atm ⁻¹)	–	–	0.0644	0.0401

^a (000)2_{1,2} → (101)3_{1,3}

^b (000)3_{2,2} → (101)3_{0,3}

1742.4 nm [12]. In this case, the broadening coefficient is about 80% larger in O₂ than in He and more than three times higher in N₂ than in He (see Table 1). Since the self- and air-broadening coefficients are similar for this R3 line and the R4 line considered in this work [13], it was assumed that foreign-broadening parameters were also similar between these two lines. For H₂O, the N₂-, O₂- and He-broadening parameters of the considered line at 1368.7 nm were also unknown. These parameters have thus been derived from the values reported for another H₂O line located at 1393.5 nm [14]. The differences in the air- and self-broadening coefficients between these two lines were about 3% and 4% for the air- and self-broadening coefficients, respectively. It was thus considered that the broadening coefficients in He, N₂ or O₂ mixtures were similar for the two lines.

The simulations performed in a He–N₂ mixture resulted in a 25% change in the 1 *f* PA signal ratio, whereas the variation in a He–O₂ mixture reached about 7%. In consequence, the maximum residual error produced by the normalization curve in mixtures of He–N₂ and O₂–He is estimated to be within 25% and 10%, respectively.

Finally, the normalization curve has been obtained with a laser that was different to the one used to measure HCl concentration, resulting in a difference in the modulation parameters. In particular, the laser frequency tuning $\Delta\nu/\Delta i$, where $\Delta\nu$ is defined above and Δi is the modulation current, changes with the modulation frequency and is laser dependent. However, since the two lasers were provided by the same manufacturer and since the operating points were similar, this effect was neglected.

3.2 Molecular relaxation

In order to investigate molecular effects of HCl in a He–N₂ mixture, the response of the sensor to 5 ppm HCl in different mixing ratios of He–N₂ was measured. Results are shown in Fig. 3. A rapid decrease of the PA signal occurs when N₂ is added to the gas mixture due to relaxation effects. For a concentration of N₂ larger than 70%, the PA signal is almost stable and reaches a value reduced by 75% in 90% of N₂ compared to the pure He mixture. These results are due to molecular relaxation effects in the HCl/He/N₂ mixture and may be explained by the energy level diagram of HCl and N₂ and by considering the deactivation pathway followed by HCl molecules excited by the laser radiation (see Fig. 4). HCl is a polar di-

TABLE 1 Parameters of the lines used in the measurements and in the simulations

atomic molecule with a vibrational mode $\tilde{\nu}_{\text{HCl}} = 2886 \text{ cm}^{-1}$. The spectroscopic properties of HCl required to understand the relaxation effects are described in [15–18] and rovibrational energy transfer processes in HCl–O₂/N₂/He are also discussed in a series of papers [19–22]. In addition, the relaxation rates for different reactions are summarized in Table 2.

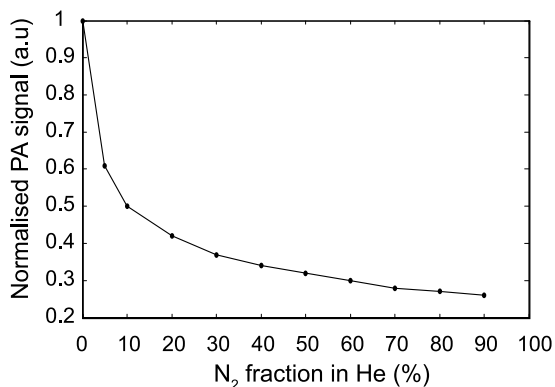


FIGURE 3 Variation of the PA signal amplitude corresponding to 5 ppm HCl as a function of N₂ fraction in He. The PA signal has been normalized by the PA signal recorded for H₂O in the same buffer gas and normalized to the value obtained in pure helium

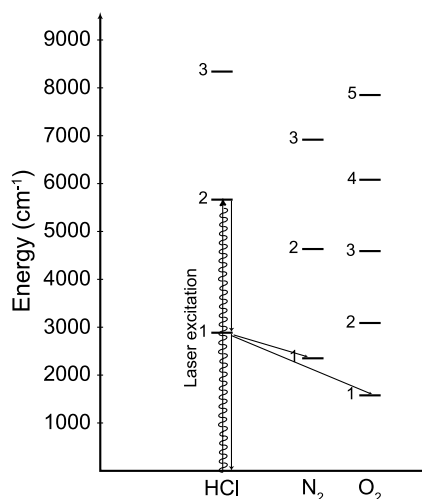


FIGURE 4 Energy level diagram of HCl and collision partners N₂ and O₂, showing the laser excitation to the $\nu = 2$ state and the subsequent relaxation scheme through V–V transfer to N₂ or O₂

Reaction	Rate ($\text{s}^{-1} \text{atm}^{-1}$)	Ref.
R_1 HCl*($\nu = 1$) + HCl \rightarrow HCl($\nu = 0$) + HCl	6.3×10^5	[22]
R_2 HCl*($\nu = 1$) + He \rightarrow HCl($\nu = 0$) + He	1.5×10^3	[19]
R_3 HCl*($\nu = 1$) + H ₂ O \rightarrow HCl($\nu = 0$) + H ₂ O	3.8×10^8	[22]
R_4 HCl*($\nu = 2$) + HCl \rightarrow HCl*($\nu = 1$) + HCl*($\nu = 1$)	7.2×10^7	[15]
R_5 HCl*($\nu = 1$) + O ₂ \rightarrow HCl($\nu = 0$) + O ₂ *($\nu = 1$)	8.1×10^4	[19]
R_6 HCl*($\nu = 1$) + N ₂ \rightarrow HCl($\nu = 0$) + N ₂ *($\nu = 1$)	6.6×10^5	[22]
R_7 N ₂ *($\nu = 1$) + N ₂ \rightarrow N ₂ ($\nu = 0$) + N ₂	1	[23]
R_8 N ₂ *($\nu = 1$) + He \rightarrow N ₂ ($\nu = 0$) + He	1.45×10^2	[24]
R_9 N ₂ *($\nu = 1$) + H ₂ O \rightarrow N ₂ ($\nu = 0$) + H ₂ O	1.1×10^5	[23]
R_{10} O ₂ *($\nu = 1$) + O ₂ \rightarrow O ₂ ($\nu = 0$) + O ₂	63	[23]
R_{11} O ₂ *($\nu = 1$) + He \rightarrow O ₂ ($\nu = 0$) + He	2.3×10^4	[25]
R_{12} O ₂ *($\nu = 1$) + H ₂ O \rightarrow O ₂ ($\nu = 0$) + H ₂ O	1.1×10^6	[26]

TABLE 2 Examples of some relaxation rates of some vibrational states of HCl with different collisional partners. Reactions labeled in *bold* correspond to V–T processes, the others to V–V processes

The principal properties are described in the following paragraph to understand, at least qualitatively, the effects of relaxation in an HCl/He/N₂ mixture. Since the laser diode emits at 1738 nm corresponding to the $\nu = 2$ vibrational state of HCl, this level is highly populated and rapid subsequent deactivation to the lower level ($\nu = 1$) occurs through collisions with N₂ and He. This transition is the most probable, since it corresponds to the smallest energy quantum. HCl molecules in the $\nu = 1$ state subsequently deactivate through collisions with He and N₂ (HCl–HCl collisions were neglected due to the low HCl concentration (< 50 ppm)). The deactivation processes ($2 \rightarrow 1$) and ($1 \rightarrow 0$) occur identically through two different pathways, one through He collisions and the other through N₂ collisions. Collisions with He molecules occur via the reaction R_2 , which is a direct V–T transfer that contributes to the PA signal. However, the relaxation time of this process, $\tau_{\text{HCl-He}} = 6.7 \times 10^{-4}$ s at a pressure of 1 atm [19], is not short enough to ensure that $\omega\tau \ll 1$ (see (1); in this case, $\omega\tau = 12$), so that the PA signal is already expected to be reduced in He. When N₂ is added to the gas mixture, according to the energy diagram, part of the released energy is transferred to the first excited state of N₂ ($\nu = 1$, $\tilde{\nu}_{\text{N}_2} = 2330 \text{ cm}^{-1}$) through a vibration-to-vibration (V–V) process, which is the most probable energy transfer. The path through N₂ is much more efficient (400 times) than through He (compare reactions R_2 and R_6), so that part of the energy initially absorbed in HCl transfers to N₂. However, the deactivation of the N₂ excited level to the ground state via V–T transfer is very slow ($\tau = 1$ s at 1 atm, see R_7), so that $\omega\tau \gg 1$. Therefore, this energy accumulates in N₂ and does not contribute to the generation of the PA signal, so that only a reduced energy $\Delta E = \tilde{\nu}_{\text{HCl}} - \tilde{\nu}_{\text{N}_2} = 555 \text{ cm}^{-1}$ takes part in the signal. The percentage of energy stored in the first excited level of N₂ ($\nu = 1$) is 80%, corresponding to $\tilde{\nu}_{\text{N}_2}/\tilde{\nu}_{\text{HCl}}$. The presence of He does not improve the relaxation of the N₂ ($\nu = 1$) state, since the relaxation time of the V–T transfer N₂–He is not small enough ($\tau_{\text{N}_2\text{-He}} = 6.9 \times 10^{-3}$ s at 1 atm, reaction R_8) to obtain the condition $\omega\tau \ll 1$.

The variation of the PA response of 5 ppm HCl in different dry mixtures of He–O₂ is shown in Fig. 5. An increase of the PA signal is first observed when increasing the O₂ concentration up to 30%. From that point, the PA signal starts to decrease and reaches, in 90% of O₂, a value close to the one in pure He. These experimental results may be explained by considering the deactivation pathway followed by HCl molecules excited by the laser radiation. The successive ($2 \rightarrow 1$) and

($1 \rightarrow 0$) deactivation of HCl is the same as explained in the preceding paragraph, the N₂ partner being replaced by O₂ molecules. Collisions with He are also the same as mentioned in the HCl/He/N₂ system.

When O₂ is added to the gas mixture, a second relaxation pathway is opened, so that excited HCl molecules deactivate through HCl–O₂ collisions as well. According to the energy diagram, part of the released energy is transferred to the first level of O₂ ($\nu = 1$, $\tilde{\nu}_{\text{O}_2} = 1556 \text{ cm}^{-1}$) through a V–V process, which is the most probable energy transfer. In this case, only the part of the energy $\Delta E = \tilde{\nu}_{\text{HCl}} - \tilde{\nu}_{\text{O}_2} = 1330 \text{ cm}^{-1}$ that is not transferred in the first excited state of O₂ directly contributes to the PA signal. Here again, the deactivation of this level to the ground state is long in the absence of He ($\tau = 1/63$ s at 1 atm, see R_{10}) compared to the modulation period, so that the energy transferred to O₂ does not contribute to the PA signal. In Fig. 5, the PA signal increases with a few percent of O₂, which can be explained as follows: the relaxation of HCl is about 50 times more efficient with O₂ collisions than with He (compare reactions R_2 and R_5), so that the V–V process with O₂ is the preferred one. In this process, only part of the energy ($\tilde{\nu}_{\text{HCl}} - \tilde{\nu}_{\text{O}_2}$) is transformed into kinetic energy contributing to the PA signal, the remaining being transferred into internal energy of O₂, which has a long relaxation time in the case of collisions with O₂. However, the presence of He plays the role of a catalyst for this relaxation (as already shown for the case of CH₄ in O₂ [4]), which drastically reduces the time decay of the O₂ excited state (see

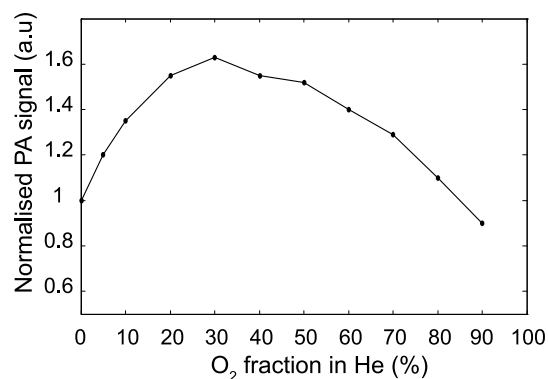


FIGURE 5 Variation of the PA signal amplitude corresponding to 5 ppm HCl as a function of O₂ fraction in He. The PA signal has been normalized by the PA signal recorded for H₂O in the same buffer gas and normalized to the value obtained in pure helium

reaction R_{11}). Therefore, the energy stored in the O_2 ($v = 1$) level deactivates fast enough to contribute to the PA signal. This two-step relaxation pathway is more efficient than the V–T process due to HCl–He collisions, which explains the initial increase of the PA signal observed when adding O_2 to He. However, when the percentage of O_2 increases more, the concentration of He is insufficient to reduce the relaxation time and the PA signal starts to decrease.

Finally, the PA signal obtained in 90% O_2 is more important than in 90% N_2 , since the part of the energy that is transferred into internal energy (to O_2 or N_2) and that is thus lost for the PA signal (due to the long relaxation time) is weaker because $\tilde{\nu}_{O_2} < \tilde{\nu}_{N_2}$.

3.3 Improvement of V–T transfers by the use of a catalyst

The efficiency of water vapor acting as a catalyst was already demonstrated for the detection of methane in the presence of oxygen [4]. The same procedure was applied to the HCl–He– O_2 and HCl–He– N_2 systems. Figure 6 shows the PA signal for a concentration of 5 ppm HCl and a varying water-vapor concentration in a mixture of 50% He–50% O_2 . The water-vapor content in the gas mixture was adjusted by passing part of the O_2 flow through a saturator, i.e. a water-filled glass cuvette placed in a thermostat bath. The flow exiting the cuvette was saturated in water vapor and the humidity was dependent only on the bath temperature. The H_2O concentration was then varied by changing the ratio dry O_2 /humid O_2 . The water-vapor concentration was continuously recorded with a commercially available hygrometer to ensure the correct concentration. The PA signal increases as soon as less than 1‰ of H_2O is added to the mixture. The effect of H_2O on the deactivation of the first level of O_2 is immediate, since the O_2 ($v = 1$) relaxation time is drastically reduced (see reaction R_{12}), which improves the generation of the acoustic wave.

A quantitative relaxation time $\tau_{O_2-H_2O}$ has been obtained by applying a fit corresponding to the equation

$$S_{PA} = S_{off} + \frac{S_0 - S_{off}}{\sqrt{1 + (\omega\tau)^2}}, \quad (1)$$

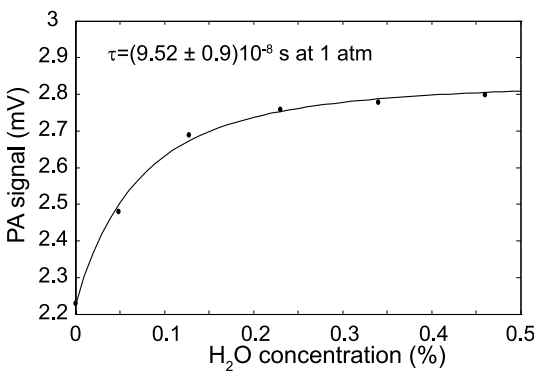


FIGURE 6 Amplitude dependence of the PA signal corresponding to 5 ppm HCl as a function of the H_2O content in the carrier gas composed of 50% O_2 and 50% He. Dots represent the measurement points and the line is the result of a fitting procedure (see text for details)

where S_{off} is the value obtained for the dry O_2 –He mixture (0% H_2O), S_0 is the full PA signal obtained in the absence of relaxation effects, ω is the angular modulation frequency and $\tau^{-1} = C_{H_2O}\tau_{O_2-H_2O}^{-1} + C_{O_2}\tau_{O_2-O_2}^{-1} + C_{He}\tau_{O_2-He}^{-1}$ is the overall relaxation rate. This fit results in a relaxation time $\tau = (9.52 \pm 0.9) \times 10^{-8}$ s at 1 atm (the error is the standard deviation given by the fitting process), which is a factor of 10 lower than the value given by reaction R_{12} ($\tau = 9.1 \times 10^{-7}$ s at 1 atm).

The same procedure was applied in the HCl–He– N_2 system (50% He–50% N_2) whose results are presented in Fig. 7. An increase of a factor of 4 of the PA signal is obtained after the addition of 0.8% of H_2O in the He– N_2 mixture. Here again, the deactivation of the first N_2 excited level is efficiently achieved due to the catalyst effect of H_2O (see reaction R_9). The effect is even more efficient in the N_2 –He mixture than in O_2 –He, since He does not act as a catalyst for N_2 . A quantitative relaxation time was extracted by the same fitting procedure as described for the He– O_2 system resulting in a relaxation time of $\tau = (1.2 \pm 0.07) \times 10^{-7}$ s at 1 atm, which is a factor of 70 smaller than the value given by reaction R_9 ($\tau = 9.1 \times 10^{-6}$ s at 1 atm).

The extracted relaxation times were in both cases much smaller than the value given in [23], probably due to the fact that the (V–T) relaxation process HCl– H_2O (see reaction R_3) was not considered in our simplified model. The very efficient corresponding rate in combination with a small fraction of water vapor can thus not be neglected in our measurements, since it opens an additional, fast relaxation pathway for the de-excitation of HCl molecules, which affects the determination of the relaxation times $\tau_{N_2-H_2O}$ or $\tau_{O_2-H_2O}$.

In order to improve the precision of our measurements, and to reduce the influence of other parameters unrelated to relaxation effects, a better normalization of the PA signal could be obtained by using the measurement of HCl in the same He– O_2 and He– N_2 mixtures, but with the addition of H_2O , as a reference. Molecular relaxation effects would therefore be suppressed in this case and the unwanted contribution due to the line-broadening parameters and to the laser frequency tuning coefficient would be avoided, since the same laser and the same absorption line would be used both for the measurement and the reference.

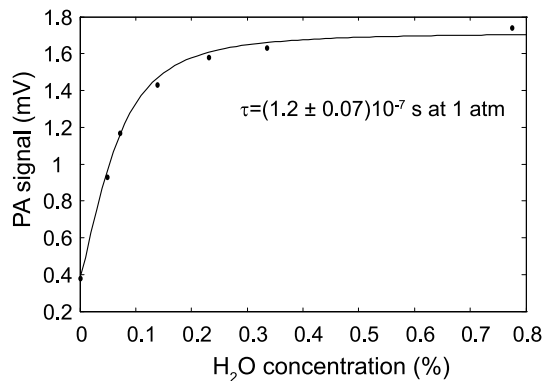


FIGURE 7 Amplitude dependence of the PA signal corresponding to 5 ppm HCl as a function of the H_2O content in the carrier gas composed of 50% N_2 and 50% He. Dots represent the measurement points and the line is the result of a fitting procedure (see text for details)

4 Conclusion

The importance of molecular relaxation in the generation of the PA signal has been demonstrated for the case of HCl detection in mixtures of He–O₂ and He–N₂. The effect on the PA signal was qualitatively explained by the use of the energy diagram of these substances and the associated relaxation rates. These two cases show the crucial importance of a proper calibration of the PA sensor, since, for example, replacing the same N₂ concentration by O₂ in helium induces a drastic change in the sensor response. In addition, the role of water vapor acting as a catalyst in both He–O₂ and He–N₂ systems was clearly identified. Finally, it was demonstrated that helium enhances the V–T transfer in the HCl–O₂ system, thus improving the generation of the PA signal.

ACKNOWLEDGEMENTS The authors would like to acknowledge NTT Electronics Corporation for providing DFB lasers.

REFERENCES

- 1 M.W. Sigrist, *Rev. Sci. Instrum.* **74**, 486 (2003)
- 2 A. Miklós, P. Hess, Z. Bozóki, *Rev. Sci. Instrum.* **72**, 1937 (2001)
- 3 P.L. Meyer, M. Sigrist, *Rev. Sci. Instrum.* **61**, 1779 (1990)
- 4 S. Schilt, J.P. Besson, L. Thévenaz, *Appl. Phys. B* **82**, 319 (2006)
- 5 A. Veres, Z. Bozóki, A. Mohácsi, M. Szakáll, G. Szabó, *Appl. Spectrosc.* **57**, 900 (2003)
- 6 A.A. Kosterev, T.S. Mosely, F.K. Tittel, *Appl. Phys. B* **85**, 295 (2006)
- 7 J.P. Besson, S. Schilt, F. Sauser, E. Rochat, P. Hamel, F. Sandoz, M. Niklès, L. Thévenaz, *Appl. Phys. B* **85**, 343 (2006)
- 8 J.P. Besson, S. Schilt, L. Thévenaz, *Spectrochim. Acta A* **63**, 899 (2006)
- 9 G. Wysocki, A.A. Kosterev, F.K. Tittel, *Appl. Phys. B* **85**, 301 (2006)
- 10 D.S. Bomse, A.C. Stanton, J.A. Silver, *Appl. Opt.* **31**, 718 (1992)
- 11 S. Schilt, L. Thévenaz, *Infrared Phys. Technol.* **48**, 154 (2006)
- 12 M. De Rosa, C. Nardini, C. Piccolo, C. Corsi, F. D'amato, *Appl. Phys. B* **72**, 245 (2001)
- 13 L.S. Rothman, D. Jacquemart, A. Barbe, D.C. Benner, M. Birk, L.R. Brown, M.R. Carleer, C. Chackerian Jr., K. Chance, L.H. Coudert, V. Dana, V.M. Devi, J.M. Flaud, R.R. Gamache, A. Goldman, J.M. Hartmann, K.W. Jucks, A.G. Maki, J.Y. Mandin, S.T. Massie, J. Orphal, A. Perrin, C.P. Rinsland, M.A.H. Smith, J. Tennyson, R.N. Tolchenov, R.A. Toth, J. Vander Auwera, P. Varanasi, G. Wagner, *J. Quant. Spectrosc. Radiat. Transf.* **96**, 139 (2005)
- 14 V. Zéninari, B. Parvitte, D. Courtois, N.N. Lavrentieva, Y.N. Ponomarev, G. Durry, *Mol. Phys.* **102**, 1697 (2004)
- 15 C.J. Dasch, C.B. Moore, *J. Chem. Phys.* **72**, 4117 (1980)
- 16 S.R. Leone, C.B. Moore, *Chem. Phys. Lett.* **19**, 340 (1973)
- 17 M.M. Hopkins, H.L. Chen, *J. Chem. Phys.* **57**, 3816 (1972)
- 18 H.L. Chen, C.B. Moore, *J. Chem. Phys.* **54**, 4072 (1971)
- 19 P.F. Zittel, C.B. Moore, *J. Chem. Phys.* **58**, 2922 (1973)
- 20 F. Al Adel, L. Doyennette, M. Margottin-Maclou, L. Henry, *J. Chem. Phys.* **77**, 3003 (1982)
- 21 D.J. Seery, *J. Chem. Phys.* **58**, 1796 (1973)
- 22 H.L. Chen, C.B. Moore, *J. Chem. Phys.* **54**, 4080 (1971)
- 23 H.E. Bass, H.J. Bauer, *Appl. Opt.* **12**, 1506 (1973)
- 24 R. Frey, J. Lukasik, J. Ducuing, *Chem. Phys. Lett.* **14**, 514 (1972)
- 25 D.R. White, R.C. Millikan, *J. Chem. Phys.* **39**, 1807 (1963)
- 26 D.R. White, *J. Chem. Phys.* **42**, 2028 (1965)